AMERICAN SOCIETY FOR MICROBIOLOGY | Microbiology Spectrum

RESEARCH ARTICLE

Superoxide Initiates the Hyphal Differentiation to Microsclerotia Formation of *Macrophomina phaseolina*

Hsien-Hao Liu,[a] Cheng-Chun Huang,[a] Ying-Hong Lin,[b] Min-Nan Tseng,[c] Hao-Xun Chang[a]

[a]Department of Plant Pathology and Microbiology, National Taiwan University, Taipei City, Taiwan
[b]Department of Plant Medicine, National Pingtung University of Science and Technology, Pingtung, Taiwan
[c]Kaohsiung District Agricultural Research and Extension Station, Council of Agriculture, Pingtung, Taiwan

ABSTRACT The infection of *Macrophomina phaseolina* often results in a grayish appearance with numerous survival structures, microsclerotia, on the plant surface. Past works have studied the development of fungal survival structures, sclerotia and microsclerotia, in the Leotiomycetes and Sordariomycetes. However, *M. phaseolina* belongs to the Dothideomycetes, and it remains unclear whether the mechanism of microsclerotia formation remains conserved among these phylogenetic clades. This study applied RNA-sequencing (RNA-Seq) to profile gene expressions at four stages of microsclerotia formation, and the results suggested that reactive oxygen species (ROS)-related functions were significantly different between the microsclerotia stages and the hyphal stage. Microsclerotia formation was reduced in the plates amended with antioxidants such as ascorbic acid, dithiothreitol (DTT), and glutathione. Surprisingly, DTT drastically scavenged H_2O_2, but the microsclerotia amount remained similar to the treatment of ascorbic acid and glutathione that both did not completely eliminate H_2O_2. This observation suggested the importance of O_2^- over H_2O_2 in initiating microsclerotia formation. To further validate this hypothesis, the superoxide dismutase 1 (SOD1) inhibitor diethyldithiocarbamate trihydrate (DETC) and H_2O_2 were tested. The addition of DETC resulted in the accumulation of endogenous O_2^- and more microsclerotia formation, but the treatment of H_2O_2 did not. The expression of SOD1 genes were also found to be upregulated in the hyphae to the microsclerotia stage, which suggested a higher endogenous O_2^- stress presented in these stages. In summary, this study not only showed that the ROS stimulation remained conserved for initiating microsclerotia formation of *M. phaseolina* but also highlighted the importance of O_2^- in initiating the hyphal differentiation to microsclerotia formation.

IMPORTANCE Reactive oxygen species (ROS) have been proposed as the key stimulus for sclerotia development by studying fungal systems such as *Sclerotinia sclerotiorum*, and the theory has been adapted for microsclerotia development in *Verticillium dahliae* and *Nomuraea rileyi*. While many studies agreed on the association between (micro) sclerotia development and the ROS pathway, which ROS type, superoxide (O_2^-) or hydrogen peroxide (H_2O_2), plays a major role in initiating hyphal differentiation to the (micro) sclerotia formation remains controversial, and literature supporting either O_2^- or H_2O_2 can be found. This study confirmed the association between ROS and microsclerotia formation for the charcoal rot fungus *Macrophomina phaseolina*. Moreover, the accumulation of O_2^- but not H_2O_2 was found to induce higher density of microsclerotia. By integrating transcriptomic and phenotypic assays, this study presented the first conclusive case for *M. phaseolina* that O_2^- is the main ROS stimulus in determining the amount of microsclerotia formation.

KEYWORDS hydrogen peroxide (H_2O_2), *Macrophomina phaseolina*, microsclerotia, reactive oxygen species (ROS), superoxide (O_2^-)

Editor Giuseppe Ianiri, University of Molise

Address correspondence to Hao-Xun Chang, hxchang@ntu.edu.tw.

The authors declare no conflict of interest.

Received 29 October 2021
Accepted 23 December 2021
Published 26 January 2022

Macrophomina phaseolina is a plant-pathogenic fungus that causes charcoal rot on a broad range of crops, including monotcuts such corn and sorghum, as well as dicots such as azuki bean and soybean (1, 2). Yield losses caused by *M. phaseolina* on soybean were reported over 3 billion bushels (3), and charcoal rot was recognized as the second most important disease of soybean in a meta-analysis of 20 years of data (2). There is no complete resistance reported for charcoal rot, but some soybean varieties were found to exhibit moderate resistance (4). In addition, disease management may rely on the conventional practices such as appropriate irrigation and fungicide treatments (5–7). As *M. phaseolina* persists in debris and soils for years by forming the survival structure microsclerotia, advanced studies on the microsclerotia formation may provide novel insights to reduce the fungal survival structures in fields.

There are different types of sclerotia-like fungal structures, such as the true sclerotia, the pseudosclerotia, the small sclerotia, and the microsclerotia. All these structures were reported to have survival capability. Among these sclerotia-like fungal structures, the first description of sclerotia was named by De Bary in studying *Sclerotinia sclerotiorum* in 1886 (8). The earliest definition of a "sclerotium" can be tracked back to the documentation provided by Ainsworth and Bisby as "a firm, frequently rounded mass of hyphae, with or without the addition of host tissue or soil, normally having no spores in or on it" (9, 10). Later, the true sclerotium depicts a specialized fungal structure with a clear and melanized outer rind to separate the middle layer of cortex and the inner layer of medulla. The true sclerotia are multilayer structures that can be 2 to 8 mm on beans (*Phaseolus vulgaris*) and 12 cm or even larger on sunflowers (*Harpalium* Cass.) (11, 12). The composition of true sclerotia contains only hyphal mass without plant tissues or soils, and the true sclerotia are capable of forming apothecia to disseminate ascospores.

The second type of sclerotia was called "pseudosclerotia," which describes the fungal survival structures with melanized and condensed mycelia, generally wrapped with plant tissues or soils (13). Fungal conidia may occur on the pseudosclerotia, which may produce apothecia to disseminate ascospores as the primary inoculum in the new season. A typical example will be the mummified survival structure of *Monilia* species on stone fruits (14). On the other hand, the third type of sclerotia was called "small sclerotia," which was first described by R.E. Smith related to lettuce infection caused by *S. sclerotiorum* (15). However, the small sclerotia was conceptualized as sclerotia of 0.5 to 2 mm, with an emphasis on its ability of infecting plants using hyphae grown out from the small sclerotia instead of forming apothecia to disseminate ascospores (16). Based on the morphological and physiological differences, the isolate was reclassified the as a new species, *Sclerotinia minor*, which becomes the species type for producing small sclerotia (17).

Similar to the observation on the small sclerotia, the fourth term "microsclerotia" describes a tiny melanized and condensed survival structure of *Verticillium* species. Different from sclerotia and small sclerotia, the development of microsclerotia was proposed to begin with a single hypha. In the case of *Verticillium dahliae*, microsclerotia formation was initiated by lateral budding on a single hypha, which becomes a spherical compact microsclerotia with melanized and hyaline cells inside (18). The inner hyaline cells were proposed to be autolyzed cells during the differentiation, and these cells may not be viable for germination (19). In the case of *M. phaseolina*, microsclerotia formation was initiated by secondary branching hyphae wrapping on the primary hypha, which develops into the globose structure. Alternatively, the primary hyphae may proliferate and protrude to increase the cell mass for microsclerotia formation (20). Different from microsclerotia of *V. dahliae*, the inner cells of *M. phaseolina* microsclerotia were found to be all melanized with capability of germination (19).

Although histological studies have categorized fungal sclerotia into at least four types aforementioned, the initiation of sclerotia formation appears to be conserved based on the studies of *Athelia rolfsii* (previously known as *Sclerotium rolfsii*), *S. minor*, *S. sclerotiorum*, and *Rhizoctonia solani*. Using these fungal systems, the theory of reactive oxygen species (ROS)-induced sclerotia development was conceptualized (21). The

theory was proposed when the concentration of malondialdehyde in the total phospholipids was measured to be higher in the center of a fungal colony, where more sclerotia formed. This observation suggested that the lipid peroxidation, an indicator of intracellular ROS stress, was associated with sclerotia formation of *A. rolfsii* (22). In addition, the oxidative stress comparison between sclerotia-forming and non-sclerotia-forming *S. sclerotiorum* strains revealed a 5-fold difference in reduced form over oxidized form of erythroascorbate (23). Subsequent studies applied antioxidants such as ascorbic acid to *A. rolfsii* (24), *S. minor* (25), *S. sclerotiorum* (23), and *R. solani* (26), and these studies consistently resulted in the reduction of sclerotia formation. The application of ROS scavengers such as benzoate and ethanol also resulted in the reduction of sclerotia formation (27). In addition, the measurement of hydrogen peroxide (H_2O_2) was found to be higher along with sclerotia development (28–30), and the addition of radical stimulator H_2O_2 increased cell proliferation and sclerotia formation in *A. rolfsii* and *S. sclerotiorum* (31). Collectively, these studies demonstrated a strong association between ROS production and sclerotia formation, and a theory of ROS-induced sclerotia development was therefore widely recognized (21).

In this theory, vegetative hyphae (an undifferentiated state) need to be stimulated by endogenous ROS stress to initiate hyphal differentiation. Similarly, protective mechanisms such as melanin synthesis and catalase activities would be upregulated to reduce the damage of ROS burst. The sclerotia development ends up with a programmed cell death and autolysis to form the O_2^--impermeable and melanized rind, while the inner medulla maintains a resting status, waiting for germination in suitable conditions (21). With the advent of high-throughput sequencing in profiling fungal transcriptomes, several studies have examined whether the theory of ROS-induced sclerotia development is universal for the microsclerotia of *V. dahliae* and *Nomuraea rileyi*. For example, a study on superoxide dismutase 1 (SOD1), catalase, and glutathione metabolism-related genes proved them to be highly expressed in microsclerotia formation of *N. rileyi* (32). In addition, one catalase (VDAG_03079) of *V. dahliae* was found to have higher expression in the microsclerotia-forming strain than the non-microsclerotia-forming strain (33). Consistently, another study reported that three catalases (VDAG_03079, VDAG_03661, and VDAG_09115) were upregulated, with VDAG_03079 being the predominant gene (34). Accordingly, these expression analyses supported that ROS burst and detoxification are associated with microsclerotia formation.

Although the theory of ROS-induced microsclerotia development has been supported using different fungal systems, these fungi all belong to the Leotiomycetes and Sordariomycetes class, while *M. phaseolina* belong to the Dothideomycetes. It remains unclear whether the mechanism of microsclerotia formation remains conserved among Leotiomycetes, Sordariomycetes, and Dothideomycetes, and it remains uncertain whether the theory of ROS-induced sclerotia development can be applied to the microsclerotia of *M. phaseolina*. As limited genetic studies have been focused on *M. phaseolina*, this study applied RNA-sequencing (RNA-Seq) to profile gene expression during the microsclerotia formation stages of *M. phaseolina*. The differential gene expression and gene ontology analysis identified ROS-related activities during the microsclerotia formation. The microsclerotia inhibition and stimulation assays were conducted and confirmed the involvement of ROS, especially for superoxide (O_2^-), as the main stimulus to initiate hyphal differentiation to microsclerotia formation of *M. phaseolina*.

RESULTS

RNA-Seq analyses for the four developmental stages of microsclerotia. The microsclerotia formation of *M. phaseolina* was categorized into four stages: the MS0 stage represented by hyaline and filamentous hyphae showing no wrapping, no swelling, or any specialized structures; the MS1 stage represented by wrapped and aggregated mycelia as the initial form of microsclerotia, but the initial microsclerotia remains white to light brown in color; the MS2 stage represented by light to dark brown microsclerotia; and the MS3 stage represented by condensed and dehydrated microsclerotia with a black appearance and reflective mucilage on the surface (Fig. 1A). Fungal tissues

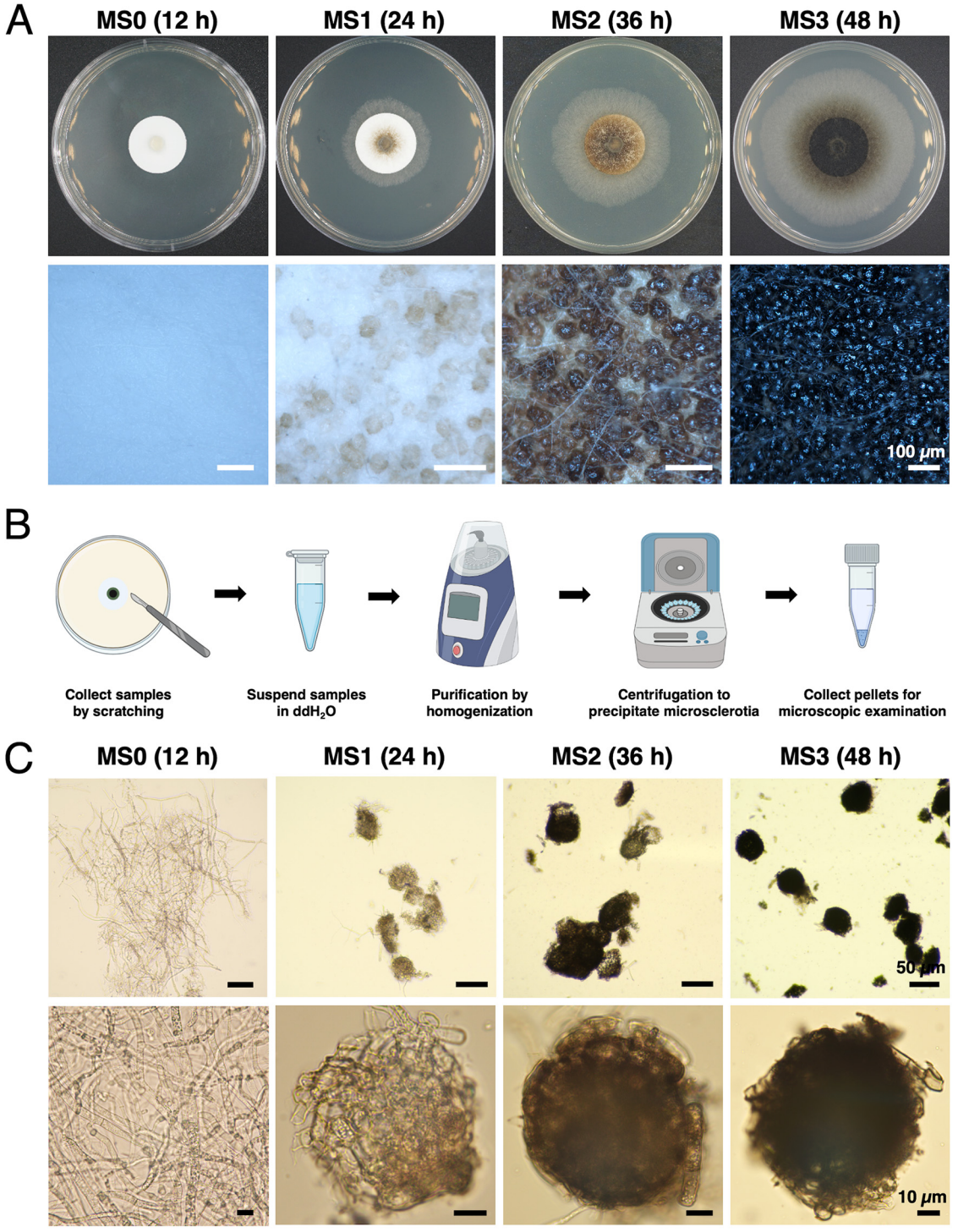

FIG 1 Microsclerotia formation and purification for *M. phaseolina*. (A) Microsclerotia formation of *M. phaseolina* categorized into four stages based on the appearance and timeline. MS0 represents the hyphae stage, which contains no pigmentation or aggregation. MS1 represents the initial stage of microsclerotia formation, during which hyphae aggregated into hyaline and spheric structures. MS2 represents the middle stage of microsclerotia formation, during which the spheric structures begin to condense and exhibit brown pigmentation. MS3 represents the mature stage of microsclerotia formation, during which the spheric structures become completely condensed and melanized with reflective mucilage in appearance. (B) Schematic workflow for collecting and purifying microsclerotia. Figures created with BioRender.com. (C) Purified microsclerotia under microscopy. Minimizing mycelia surrounding microsclerotia or attaching on the surface of microsclerotia would provide better representation for the expression patterns in RNA-Seq results. ddH_2O, double-distilled water.

from the four stages of microsclerotia formation were collected at 12, 24, 36, and 48 h postinoculation (hpi). In order to obtain pure microsclerotia of each stage and to minimize the contamination of hyphae surrounding microsclerotia or attached on the surface of microsclerotia, a cleanup workflow was developed to ensure the purity of microsclerotia in each stage (Fig. 1B). Three biological replicates of the hyphae from the MS0 stage, as well as the purified microsclerotia from the MS1, MS2, and MS3 stages, were collected for RNA preparation (Fig. 1C).

The RNA-Seq analyses resulted in a clear sample separation in the principal-component analysis (PCA) (Fig. 2A; Table S1). The Jensen-Shannon divergence analysis suggested that the samples of MS0 and MS1 had a closer expression pattern, while the samples of MS2 and MS3 had a closer expression pattern (Fig. 2B). These results indicated that the sample purity and experimental setup were qualified for downstream studying the differential gene expressions between the stages of microsclerotia formation. Among 13,443 transcripts in the reference transcriptome, there were 12,241 transcripts detected in the RNA-Seq samples. The hierarchical clustering for these 12,241 transcripts identified six expression patterns, including 1,800, 3,220, 1,140, 2,761, 764, and 2,556 transcripts for clusters I to VI, respectively (Table S2 to S7). Among these six clusters, ROS-related transcripts could be found in clusters I, II, IV, and VI (Fig. 2C).

Cluster I contained transcripts that in general became upregulated in the MS1, MS2, and MS3 stages compared to the MS0 stage. ROS-related transcripts such as Al1_v1_10208 (glutathione *S*-transferase) and Al1_v1_11460 (glutaredoxin) were grouped in this cluster. The cluster II contained transcripts that in general became upregulated in the MS2 and MS3 stage compared to the MS0 stage, and the ROS-related transcripts such as Al1_v1_02200 (catalase) and Al1_v1_12892 (catalase) were grouped in this cluster. On the other hand, cluster IV contained transcripts that in general became downregulated in the MS2 and MS3 stage compared to the MS0 stage, and ROS-related transcripts such as Al1_v1_01834 (superoxide dismutase 1) and Al1_v1_08083 (NADH-ubiquinone oxidoreductase) were grouped in this cluster. Lastly, the cluster VI contained transcripts that in general became downregulated in the MS1, MS2, and MS3 stages compared to the MS0 stage. ROS-related transcripts such as Al1_v1_11257 (lignin peroxidase) and Al1_v1_00390 (lignin peroxidase) were grouped in this cluster.

Subsequently, differential expression analyses were performed, and the results showed that there were 2,781, 3,314, and 3,134 transcripts being upregulated in the MS1, MS2, and MS3 over the MS0 stage, respectively. On the other hand, there were 2,651, 2,955, and 2,897 transcripts being downregulated in the MS1, MS2, and MS3 over the MS0 stage, respectively (Table S8 to S10). Venn diagram analysis identified that there were 1,683 transcripts being upregulated in all three comparisons (Fig. 3A), while there were 1,552 transcripts being downregulated in all three comparisons (Fig. 3B). To further understand functional enrichment on these consensus upregulated and downregulated transcripts, gene ontology (GO) analysis was applied, and the results identified several significant biological, molecular, and cellular categories (Table S11 and S12). For the consensus upregulated transcripts, functions such as oxidoreductase activity and glutathione transferase activity were found to be significantly enriched. Other functions, such as the NAD or NADP as acceptor, were also found to be enriched in the upregulated transcripts (Fig. 3C). On the other hand, the NADH dehydrogenase (quinone) activity in the downregulated transcripts was found to be significant, indicating that potential electron-changing functions were active during the microsclerotia formation (Fig. 3D). These results suggested that ROS-related activities and functions were associated with microsclerotia formation of *M. phaseolina*.

Antioxidant inhibition assay for microsclerotia formation. To further validate the importance of ROS in the microsclerotia formation of *M. phaseolina*, antioxidants including ascorbic acid, DTT, and glutathione were selected to evaluate the effects of antioxidants on the microsclerotia formation. Serial concentrations of these antioxidants were amended into potato dextrose agar (PDA) with no negative impact on the fungal growth regardless of the concentrations (Fig. 4A). However, microsclerotia formation in the PDA plates amended with these antioxidants was reduced (Fig. 4B).

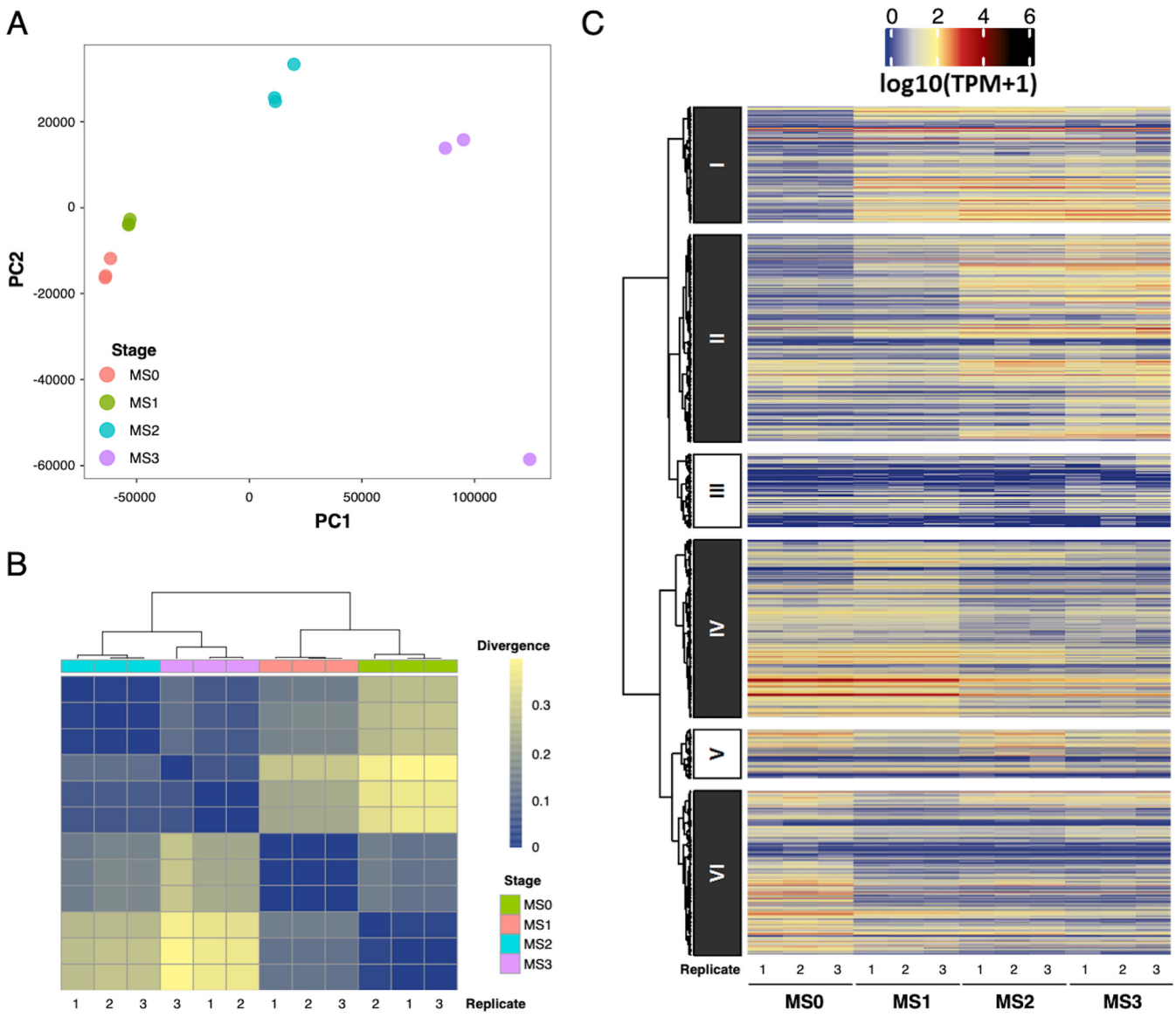

FIG 2 Principal-component analysis (PCA), Jensen-Shannon divergence heat map, and hierarchical clustering for *M. phaseolina* transcripts. (A) PCA of 12 RNA-Seq samples showed clear separation among four development stages, which indicated good quality of these samples for comparing differential gene expressions between stages. The eigenvalues of PC1 and PC2 were 89.95% and 5.78%, respectively. (B) Jensen-Shannon divergence heat map of RNA-Seq samples based on transcripts per millions (TPM). Lower divergence values represent higher similarity. The transcripts expressed in the hyphae stage and the MS1 stage were closer to each other, while the transcripts expression in the MS2 and MS3 stages were closer to each other. (C) Expression clustering for 12,241 transcripts resulted in six clusters with different expression patterns. Transcripts in clusters I, II, IV, and VI contained reactive oxygen species (ROS)-related functions. While transcripts in clusters I and II were generally upregulated in the later development stages, transcripts in clusters IV and VI were generally downregulated in to the later development stages.

Using the ImageJ quantification and simple linear regression, the 50% inhibition concentration was estimated at 5.5 mM for ascorbic acid, 1 mM for DTT, and 4.5 mM for glutathione, respectively (Fig. 4C).

Other than image analyses on the microsclerotia formation, nitro blue tetrazolium (NBT) and 3,3′-diaminobenzidine (DAB) staining were applied to visualize the amount of O_2^- and H_2O_2 in the MS1 stage, respectively (35, 36). At the 50% inhibition rate of microsclerotia formation, the intensity of NBT and DAB were consistently less than the controls, which confirmed that these three antioxidants indeed exhibited ROS scavenging capability. Surprisingly, the DAB staining for H_2O_2 in the DTT-amended samples was much lighter than the staining for ascorbic acid- and glutathione-amended samples. However, the NBT staining for O_2^- in samples of ascorbic acid-, DTT-, or glutathione-amended samples showed no

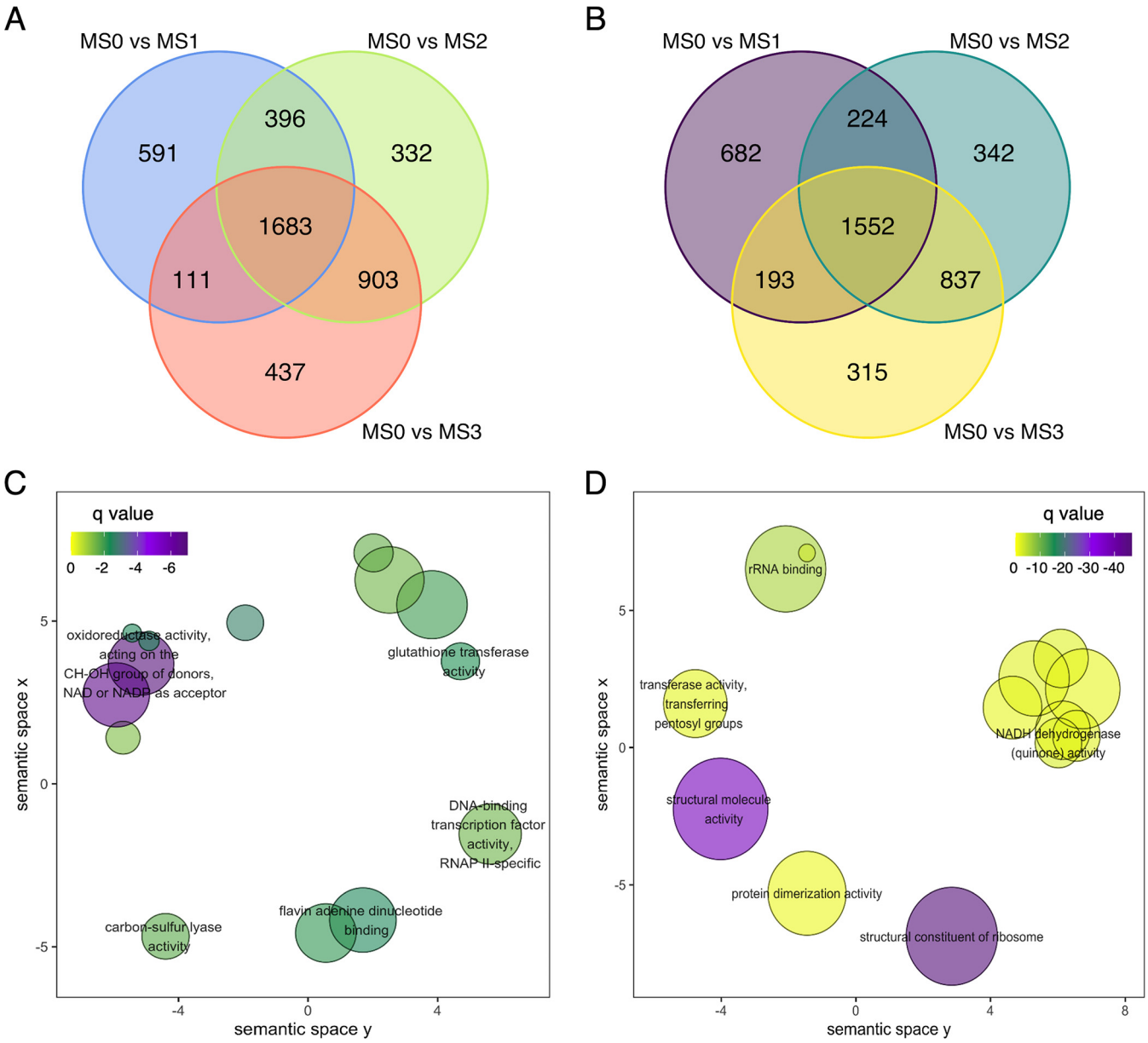

FIG 3 Venn diagram and gene ontology (GO) enrichment of the differential expressed transcripts between the microsclerotia formation stages. (A) Significant upregulated transcripts in the MS1, MS2, and MS3 stages versus the MS0 hyphae stage, respectively. There were 1,683 consensus transcripts found in the three comparisons. (B) Significant downregulated transcripts in the MS1, MS2, and MS3 stages versus the MS0 hyphae stage, respectively. There were 1,552 consensus transcripts found in the three comparisons. (C) GO enrichment for the 1,683 consensus upregulated transcripts identified ROS-related functions such as oxidoreductase and glutathione transferase activities. (D) GO enrichment for the 1,552 consensus downregulated transcripts identified fewer ROS-related functions, such as NADH dehydrogenase activity.

difference (Fig. 5). Because DTT treatment resulted in less H_2O_2 (lower intensity of DAB staining) but not a lesser amount of microsclerotia, the importance of H_2O_2 in determining the amount of microsclerotia may be minor. In other words, as long as the O_2^- concentration remained identical, the microsclerotia inhibition rate could be identical at 50% for three antioxidants (Fig. 5).

O_2^- and H_2O_2 stimulation assay for microsclerotia formation. In order to further confirm the contribution of O_2^- and H_2O_2 in determining the amount of microsclerotia formation, the Zn/Cu superoxide dismutase SOD1 inhibitor sodium diethyldithiocarbamate trihydrate (DETC) and H_2O_2 were amended to provide the ROS stress, specifically for increasing O_2^- and H_2O_2, respectively. Different concentrations of DETC and H_2O_2 were evaluated in PDA to determine the highest concentration that can be amended

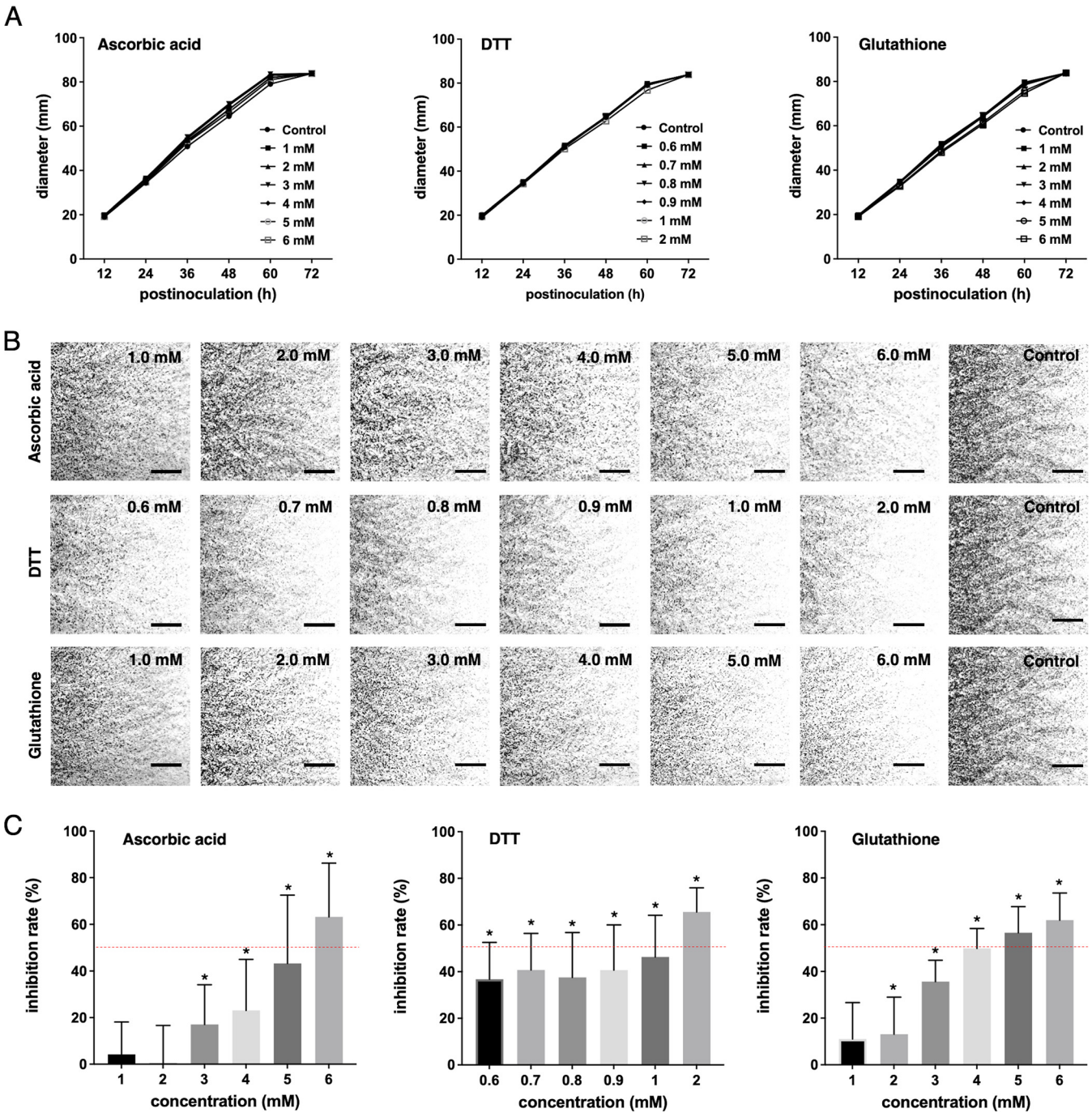

FIG 4 Microsclerotia inhibition assay on the antioxidant-amended PDA plates. (A) Serial concentrations of ascorbic acid, dithiothreitol (DTT), and glutathione were tested, and none of these concentrations showed a negative impact on the mycelia growth rate. (B) Microscopic examination for the microsclerotia formation. (C) Microsclerotia inhibition can be observed when the concentration was higher than 3 mM for ascorbic acid, 0.6 mM for DTT, and 2 mM for glutathione. The asterisks indicate statistical significance at $\alpha = 0.05$ using *t* test by comparing each concentration to the control. The 50% microsclerotia inhibition (red dashed line) was estimated at 5.5 mM for ascorbic acid, 1 mM for DTT, and 4.5 mM for glutathione, respectively. The experiments contained three repeats, and each repeat contained three biological replicates.

without harming fungal growth. However, both DETC and H_2O_2 caused growth rate reduction in a concentration-dependent manner. Among the tested conditions, H_2O_2 at 1 mM showed no significant difference from the control (Fig. 6A). On the other hand, the concentrations of 0.1, 0.2, and 0.3 mM caused the same level of growth reduction but no significant difference among these three concentrations (Fig. 6B). As

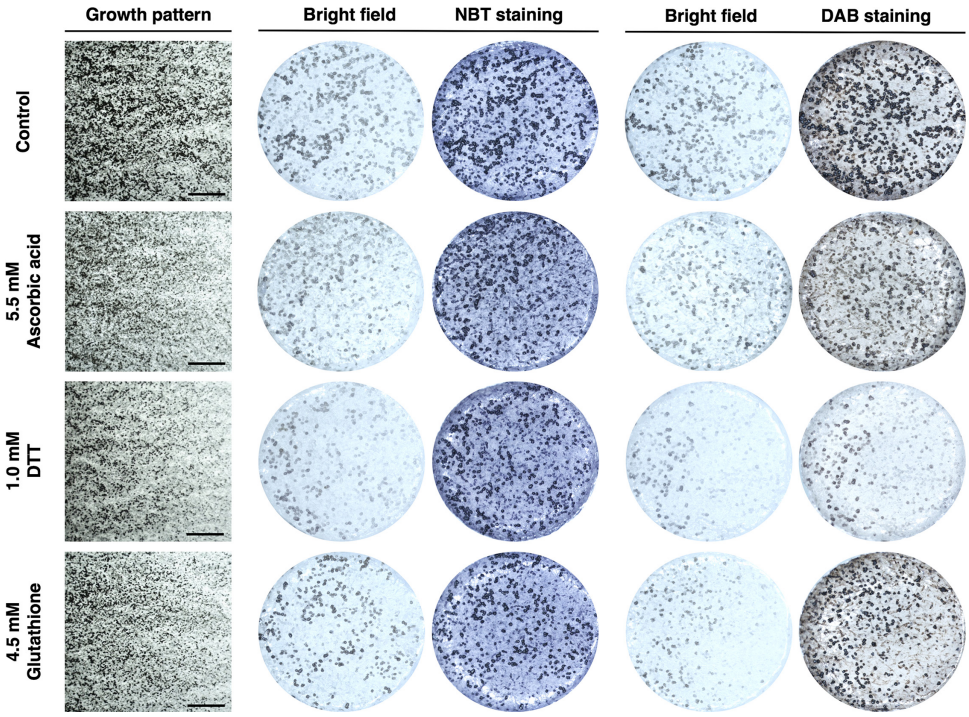

FIG 5 Nitro blue tetrazolium (NBT) staining for O_2^- and 3,3′-diaminobenzidine (DAB) staining H_2O_2 at 50% microsclerotia inhibition on the ascorbic acid-, DTT-, and glutathione-amended potato dextrose agar (PDA) plates. The 5-mm plugs were sampled at 3.5 cm from the center of a 9-cm petri dish for photographing before and after staining. The bars indicate 1 mm. Each staining was repeated two times with three independent biological replicates. At a 50% microsclerotia inhibition rate, the DAB intensity in DTT-amended samples was consistently lower than on ascorbic acid- and glutathione-amended samples, which indicated that lesser amounts of H_2O_2 did not impair the microsclerotia formation.

lower concentrations still exhibited negative impacts on mycelial growth, DETC at 0.3 mM was selected to observe its effects on the microsclerotia formation. The growth rate for *M. phaseolina* was measured at 1.29 ± 0.02, 1.27 ± 0.04, and 1.03 ± 0.02 mm/h on the control PDA plates, on the 1 mM $H_2O_2^-$ amended plates, and on the 0.3 mM DETC-amended plates, respectively. In order to compensate the reduction of growth rate, the experiments were recorded at 72 hpi for control and 1 mM H_2O_2-amended plates and 84 hpi for 0.3 mM DETC-amended plates. At these time points, the mycelia were about covered the whole 9-cm petri dish. In addition, these plates were prolongedly cultured to double confirm the final amount of microsclerotia after 7 days.

The 0.3 mM DETC-amended plates increased microsclerotia formation, while the 1 mM H_2O_2-amended plates showed no significant difference to the control (Fig. 6C). When the growth of *M. phaseolina* covered the DETC-amended PDA plate, microsclerotia formation showed high density and a wider melanized zone compared to the control, and the increased amount of microsclerotia was further confirmed after 7 days. On the other hand, the microsclerotia formation of *M. phaseolina* on the H_2O_2-amended PDA plate showed no clear difference to the control at 72 hpi, but a clear reduction of microsclerotia could be observed after 7 days (Fig. 6D). Furthermore, the DAB staining confirmed that the addition of SOD1 inhibitor DETC was functional to block the metabolic conversion from O_2^- to H_2O_2, and the intensity of H_2O_2 was much less compared to the H_2O_2-amended samples and controls (Fig. 6E). However, the microsclerotia formation was increased in the DETC-amended plates. Consistent with the ROS antioxidant inhibition assay, these results supported the role of O_2^-, but not H_2O_2, in initiating the differentiation from hyphae to microsclerotia formation.

Expression patterns of ROS-related genes in the four microsclerotia formation stages. With the knowledge that O_2^- initiates hyphal differentiation to microsclerotia of *M. phaseolina*, transcripts with ROS-related function in the ROS detoxification pathways were further evaluated. It has been shown that the O_2^- stress could be produced

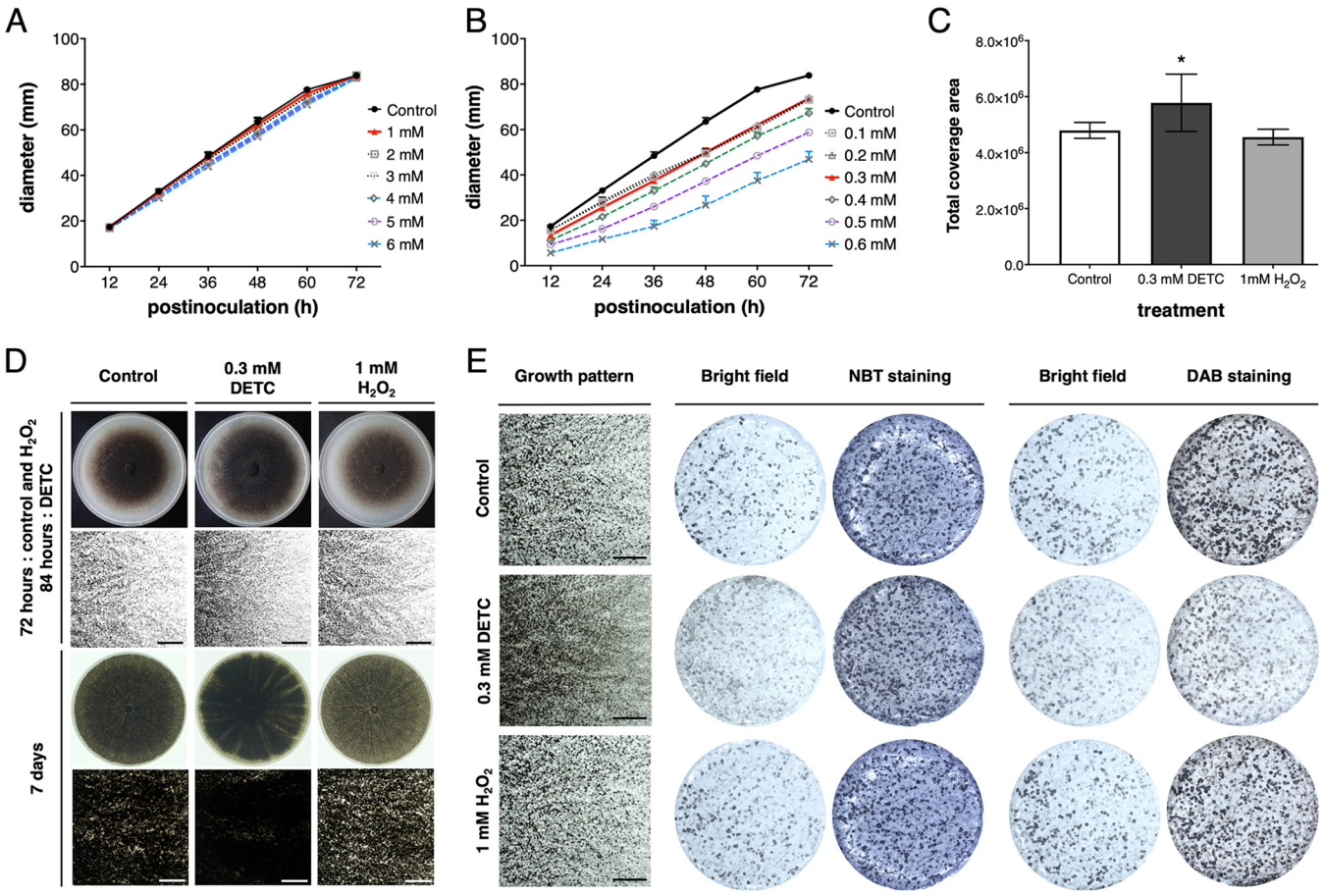

FIG 6 Microsclerotia stimulation assay supported that O_2^- stimulates microsclerotia formation in *M. phaseolina*. (A) Mycelial growth rate at different concentrations of H_2O_2-amended PDA plates. (B) Mycelial growth rate at different concentrations of diethyldithiocarbamate trihydrate (DETC)-amended PDA plates. The best concentration was defined as the highest concentration not affecting mycelial growth, as indicated by the red line, which was 0.3 mM for DETC and 1 mM for H_2O_2. (C) Microsclerotia stimulation rate of 0.3 mM DETC and 1 mM H_2O_2. An increase of microsclerotia formation of approximately 10% was estimated in 0.3 mM DETC-amended PDA plates. (D) Microsclerotia formation in a plate and in the area 3.5 cm from the center of a 9-cm petri dish. The DETC treatment stimulated high microsclerotia formation. Three biological replicates were included in each experimental repeat, and the experiment was repeated three times. The bars indicate 1 mm. (E) 5-mm plugs were sampled at the 3.5 cm from the center of a 9-cm petri dish for photographing before and after staining. The bars indicate 1 mm. Each staining was repeated three times, and each included three independent biological replicates. Because DETC blocks the process of O_2^- into H_2O_2 without reducing microsclerotia formation, the results support that O_2^- is the main ROS stimulus for microsclerotia formation in *M. phaseolina*.

by the enzymes in the mitochondrial electron transport chain such as the cytochrome *c* oxidases and NADH-ubiquinone-related oxidoreductases (37, 38). There were four cytochrome *c*-related transcripts, including cytochrome *c* (Al1_v1_05222), cytochrome *c* oxidase subunit IV (Al1_v1_06022), cytochrome *c* oxidase Va (Al1_v1_06721), and ubiquinol-cytochrome *c* reductase Fe-S subunit (Al1_v1_11781), as well as two NADH-ubiquinone oxidoreductases (Al1_v1_07068 and Al1_v1_12148) that exhibited the highest expression at the MS0 stage (Fig. 7A; Table S13). In addition, the O_2^- stress may be produced by membrane-associated enzymes such as NADPH oxidases, xanthine oxidases, and alternative oxidases (39). There were four NADPH oxidases (Al1_v1_00886, Al1_v1_05404, Al1_v1_07624, and Al1_v1_10085), xanthine oxidase (Al1_v1_08915), and alternative oxidase (Al1_v1_05095), which also showed the highest expression at the hyphal stage (Fig. 7B). The observation supported the results that O_2^- stress accumulated at the MS0 to MS1 stage to stimulate microsclerotia formation and determining the amount of microsclerotia being formed. Upon the completion of hyphae aggregation at the MS1 stage, detoxification of O_2^- and H_2O_2 stress would be needed.

To detoxify O_2^- stress, the Zn/Cu SOD1 has been shown to process O_2^- into H_2O_2 (40, 41). There were two Zn/Cu SOD1 genes (Al1_v1_01834 and Al1_v1_06322) in the *M.*

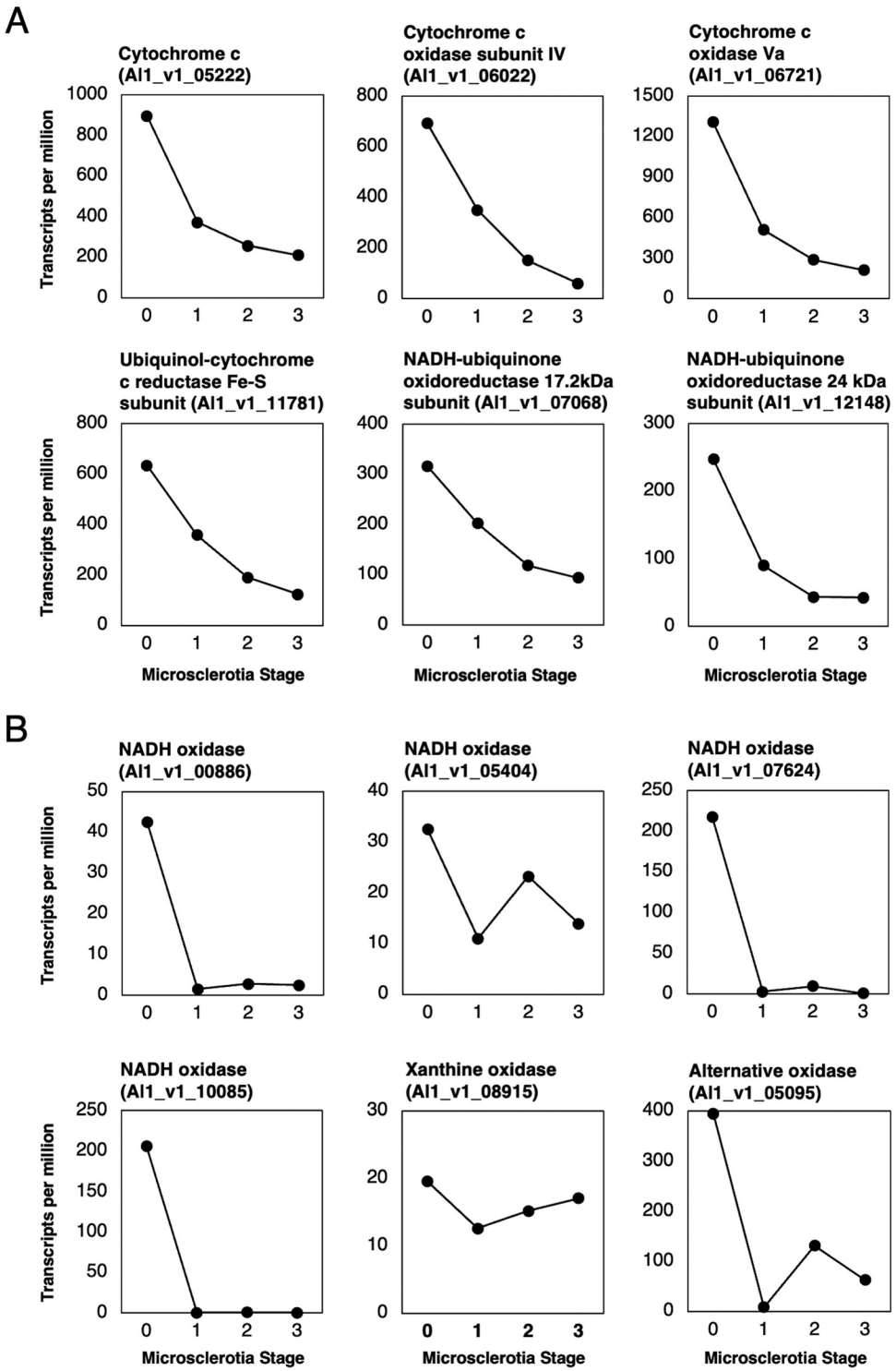

FIG 7 Expression patterns of transcripts that may generate O_2^- during microsclerotia formation. (A) Cytochrome *c* and NADH-ubiquinone oxidoreductase are known to involve in the electron transport chain to generate O_2^-. Six transcripts annotated as cytochrome *c* or NADH-ubiquinone oxidoreductase were found to have higher expression in the MS0 stage. (B) NADPH oxidase, xanthine oxidase, and alternative oxidase are also known to involve in the generation of O_2^-. Six transcripts annotated as NADPH oxidase, xanthine oxidase, or alternative oxidase exhibited higher expression in the MS0 stage. These results indicated that O_2^- generation needs to be active before the initial stage of microsclerotia formation.

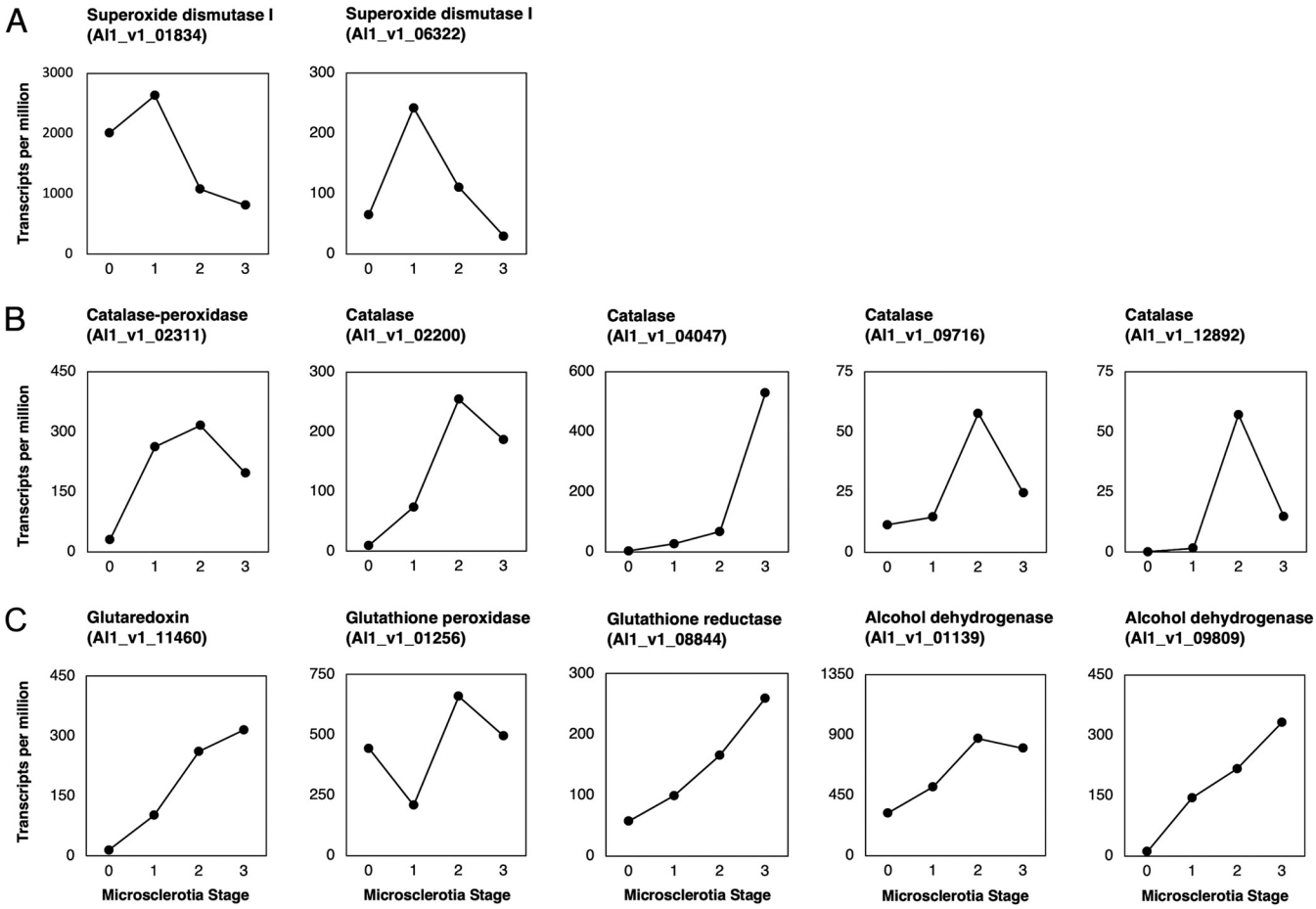

FIG 8 Expression patterns of transcripts that may detoxify O_2^- or H_2O_2 during microsclerotia formation. (A) Two transcripts annotated as superoxide dismutase 1 exhibited highest expression at the MS1 stage, which indicated that the O_2^- stress was higher at the MS0 to MS1 stage. (B) Five transcripts annotated as catalases showed higher expression toward the MS2 or MS3 stage, which indicated that the H_2O_2 stress was higher after the MS1 stage. (C) Glutaredoxin in the glutaredoxin pathway and four transcripts in the glutathione pathway were also found to have higher expression toward the MS2 or MS3 stage, which supported the H_2O_2 stress being higher at later stages.

phaseolina genome, and both genes reached the highest expression at the MS1 stage and gradually dropped down at the MS2 and MS3 stages. The phenomenon indicated that the O_2^- stress was high at the MS0 to MS1 stages, and therefore, two Zn/Cu SOD1 genes needed to be upregulated to convert O_2^- into H_2O_2 (Fig. 8A). On the other hand, it has been shown that catalases, the glutaredoxin pathway, and the glutathione pathway could reduce H_2O_2 stress (42). There were one catalase-peroxidase (Al1_v1_02311) and four catalases (Al1_v1_02200, Al1_v1_04047, Al1_v1_09716, and Al1_v1_12892), and these five genes reached the highest expression at the MS2 or MS3 stage, which suggested that H_2O_2 stress was higher after the MS1 stage (Fig. 8B). In addition, five enzymes, including glutaredoxin (Al1_v1_11460), glutathione peroxidase (Al1_v1_01256), glutathione reductase (Al1_v1_08844), and two alcohol dehydrogenases (Al1_v1_01139 and Al1_v1_09809), were also upregulated at the MS2 or MS3 stage (Fig. 8C). These results supported the possibility that the H_2O_2 stress comes after the MS1 stage, and therefore O_2^- serves as the initial ROS stimulus to initiate hyphal differentiation into microsclerotia for *M. phaseolina*. After the hyphal aggregation and the formation of hyaline microsclerotia, the O_2^- detoxification by SOD1 and H_2O_2 detoxification by catalases and enzymes in the glutaredoxin pathway and glutathione pathway became active to relieve downstream ROS stresses (Fig. 9).

DISCUSSION

Sclerotia or microsclerotia formation is a survival strategy for plant-pathogenic fungi such as *S. sclerotiorum*, *S. minor*, *V. dahliae*, and *M. phaseolina*. Advanced studies

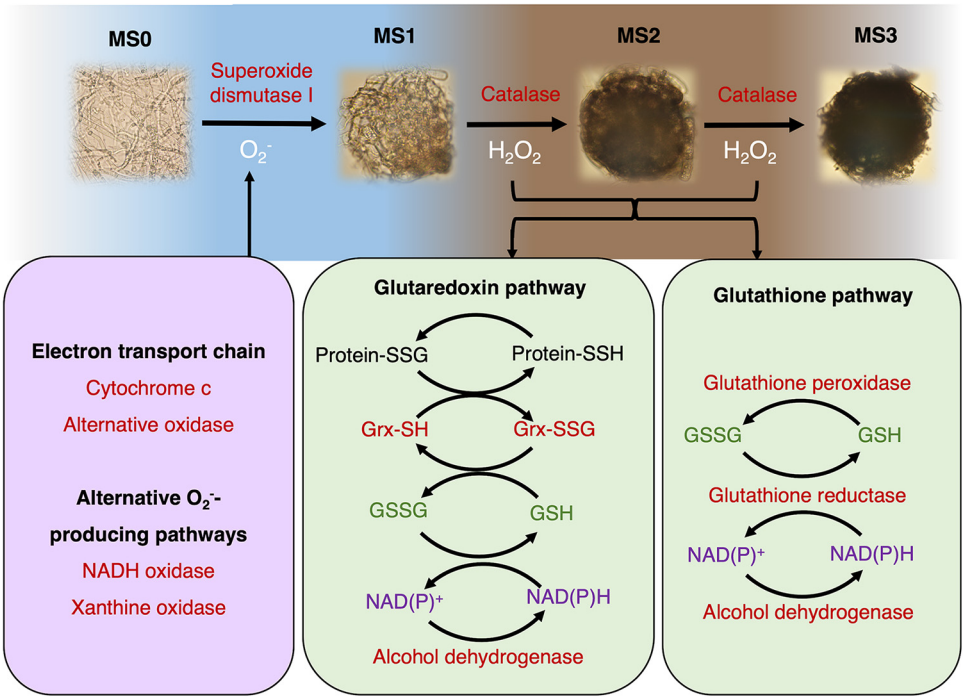

FIG 9 The schematic model for ROS metabolism during microsclerotia formation of *M. phaseolina*. O_2^- generated from electron transport chain and alternative pathways serves as the main ROS stimulus to initiate hyphal differentiation into the initial stage of microsclerotia formation (MS1). O_2^- detoxification is mediated by superoxide dismutase I, which converts O_2^- to H_2O_2. The accumulation of H_2O_2 in the middle stage of microsclerotia formation (MS2) may facilitate development into the mature stage of microsclerotia (MS3). Downstream metabolisms, including melanin synthesis and H_2O_2 detoxification through catalases, glutaredoxin pathway, and glutathione pathway, will be upregulated to prevent ROS damage to the resting fungal tissues.

on the sclerotia and microsclerotia biology are desired in order to better manage these soilborne diseases by reducing the pathogen inoculum surviving in debris and soils (5, 43, 44). Although the theory of ROS-induced sclerotia development has been supported by studying Leotiomycetes and Sordariomycetes using transcriptomic analysis and ROS inhibition assay, the theory in microsclerotia of *V. dahliae* and *N. rileyi* has been evaluated only using transcriptomic analyses; ROS inhibition and stimulation assay in the microsclerotia formation have been lacking. Moreover, *M. phaseolina* belongs to the Dothideomycetes, which is different from *V. dahliae* and *N. rileyi*, that both belong to the Sordariomycetes. Therefore, it remained unclear whether ROS stimulation remains conserved for the microsclerotia formation in *M. phaseolina*. This study applied RNA-Seq to profile four stages of microsclerotia formation in *M. phaseolina*, and the expression analyses identified that ROS-related transcripts were differentially expression during the microsclerotia formation stages. Using the ROS inhibition assay and stimulation assay, this study further demonstrated that O_2^- is the main ROS stimulus to initiate hyphal differentiation for microsclerotia formation of *M. phaseolina*.

Studies supporting that ROS generation upstream of O_2^- and H_2O_2 is involved in sclerotia and microsclerotia formation. There are several pieces of evidence to support that the generation of O_2^- and H_2O_2 are important for sclerotia and microsclerotia formation. For example, NADPH oxidase (Nox) homologs are conserved in eukaryotic cells, and the Nox family has been widely recognized for generating O_2^-. Two studies reported that mutants of *S. sclerotiorum* NADPH oxidases (SsNox1 and SsNox2) resulted in less sclerotia formation (45, 46). A similar phenomenon was observed for *Botrytis cinerea*, and the deletion mutants of either BcNoxA or BcNoxB exhibited no sclerotia (47, 48). The *N. rileyi* NrNOX-silenced mutants showed less microsclerotia formation and decreased H_2O_2 accumulation (49). For the *V. dahliae* NoxA mutants, reduction of microsclerotia formation was also observed (50). However, the product of Nox may differ depending on the homologous lineage, and it has been suggested that the

main product of Nox1, Nox2, Nox3, and Nox5 is O_2^-, while the main product of Nox4 is H_2O_2 (39). Moreover, the function of Nox may vary depending on the cellular location. For example, other research studying *B. cinerea* suggested that BcNoxA/B on the endoplasmic reticulum produces H_2O_2, while BcNoxA and BcNoxB on the plasma membrane generate O_2^- and H_2O_2, respectively (51). Moreover, NBT staining in BcNoxA/B double mutant resulted in similar NBT intensity, which indicated that additional pathways may have functional redundancy to BcNoxA/B in generating O_2^- (45). Because the conversion of O_2^- to H_2O_2 in the ROS detoxification pathway is dynamic, studies on the upstream genes such as Nox will interfere with both O_2^- and H_2O_2 simultaneously. Therefore, a better experimental strategy may be evaluating the detoxification of O_2^- and H_2O_2 by characterizing SOD1 and catalases.

Studies supporting O_2^- as the main stimulus for sclerotia and microsclerotia formation. In studying the sclerotia formation of other fungi such as *S. minor* and *S. sclerotiorum*, one study showed that sclerotia formation was reduced by adding SOD mimetics, which convert O_2^- into H_2O_2. In other words, sclerotia formation was reduced if O_2^- was decreased (29). In measuring the O_2^- concentration and the xanthine oxidase-derived O_2^-, it was found that O_2^- concentration was consistently higher in sclerotia-forming isolates than non-sclerotia-forming isolates (28, 30). Consistently, a study showed that *S. minor* growth on the H_2O_2-amended PDA did not result in more sclerotia (52).

One study observed that the mutants of *S. sclerotiorum* SOD1 (SsSOD1, SS1G_00699) showed no impairment on the sclerotia formation (53), which indicated that the elimination of H_2O_2 had no negative impact on sclerotia formation. In addition, two studies silencing catalases of *S. sclerotiorum*, which conceptually increased H_2O_2 accumulation, turned out to reduce sclerotia formation. In silencing the SsCat1 (SS1G_02784), the mutants showed slower and smaller sclerotia formation (54), and in silencing the SsCat2 (SS1G_00547), a reduced number of sclerotia was observed, although the size and weight of the sclerotia appeared to be normal (55). A similar effect was found in *Aspergillus flavus*, for which the increase of SOD expression and decrease of catalase expression in the *veA* mutant, or applying SOD mimetic TIRON and catalase inhibitor aminotriazole to the wild-type strain, all resulted in the accumulation of H_2O_2 with no sclerotia formation (56).

Other than increasing H_2O_2 accumulation by silencing catalases, in silencing other H_2O_2 detoxification mediators, including the *S. sclerotiorum* thioredoxin1 SsTrx1 (SS1G_08534) and thioredoxin reductase SsTrr1 (SS1G_05899), both mutants exhibited higher sensitivity and less capability to handle exogenous H_2O_2. The results also showed a consistent reduction of the sclerotia number in the SsTrx1-silenced and the SsTrr1-silenced mutants, which indicated that the accumulation of H_2O_2 may not promote sclerotia formation (57, 58). Accordingly, these studies suggested the possibility of O_2^- but not H_2O_2 in stimulating and determining the number of sclerotia and microsclerotia formation.

Studies supporting H_2O_2 as the main stimulus for sclerotia and microsclerotia formation. However, there are also several articles that suggested H_2O_2 was important for sclerotia formation, including studies on *A. flavus*, *R. solani*, *S. sclerotiorum*, *S. minor*, *A. rolfsii*, and *N. rileyi* (29, 31, 45). Moreover, in contrast to the knockout study of SsSOD1 (53), a study showed a reduced sclerotia formation when the same SsSOD1 was silenced and when *S. sclerotiorum* was grown on the DETC-amended PDA plates (59). These results suggested that blocking the generation of H_2O_2 resulted in no sclerotia formation, and that the application of exogenous H_2O_2 stimulated more sclerotia formation for *S. sclerotiorum* has also been documented (31). Specifically for microsclerotia formation, a recent study on the *V. dahliae* SOD1 (VdSOD1) revealed its importance as a secretory protein in scavenging both exogenous and endogenous O_2^-, but the phenotype of microsclerotia formation was not described in the VdSOD1 mutants (60).

On the other hand, a study on knocking out *A. flavus* catalase CTA1 resulted in an increased number of sclerotia, which suggested the accumulation of H_2O_2 promoted sclerotia formation (61). Another study silencing the cinnamyl alcohol dehydrogenase of *S. sclerotiorum* (SsCAD) caused the downregulation of SsNox1 and SsNox2, and less sclerotia formation was observed. The sclerotia formation was partially recovered when the SsCAD-silenced mutant was grown on the 6 mM H_2O_2-amended PDA plates,

indicating the importance of H_2O_2 in stimulating sclerotia formation. However, this study also reported the recovery was better in the 0.2 M NADPH-amended PDA plates, which suggested that a fully functional O_2^- to H_2O_2 detoxification pathway can rescue sclerotia formation better than supplying H_2O_2 alone (62).

O_2^- as the main stimulus for initiating hyphal differentiation into microsclerotia of *M. phaseolina*. While many studies have provided evidence for the importance of O_2^- or H_2O_2 in the sclerotia or microsclerotia formation in studying different Leotiomycetes and Sordariomycetes, this study integrated not only transcriptomic analyses, but also the ROS inhibition and stimulation assay to support the involvement of ROS-related activities during the microsclerotia formation of *M. phaseolina* in the Dothideomycetes class. Moreover, by using NBT staining for O_2^- and DAB staining for H_2O_2, this study provided a direct visualization for the importance of O_2^- in determining the amount of microsclerotia formation. As *M. phaseolina* growing on the SOD1 inhibitor DETC-amended PDA plates resulted in more microsclerotia formation, but not *M. phaseolina* growing on the H_2O_2-amended PDA plates, the results provided direct supports for O_2^- as the main ROS stimulus in initiating microsclerotia formation of *M. phaseolina*. The results also suggested that the ROS stimulation mechanism or ROS signal may remain conserved in the evolution between Leotiomycetes, Sordariomycetes, and Dothideomycetes. Future studies would further resolve the details in O_2^- and/or H_2O_2 reception and additional mechanisms involved in the sclerotia- or microsclerotia-forming capability of plant-pathogenic fungi.

MATERIALS AND METHODS

Fungal material and microsclerotia preparation. *M. phaseolina* isolate a31 was routinely maintained on PDA in dark at 28°C. The Mycelia blocks from actively growing margins of colonies were inoculated on PDA covered with a 0.45-μm nylon membrane (Pall Corporation, Ann Arbor, MI). Sample collection was completed at four stages of microsclerotia formation. The first stage (MS0) collected the mycelia at 12 h postinoculation (hpi) from potato dextrose broth after filtering mycelia through a double layer gauze with twice washing using sterile water. The second stage (MS1), third stage (MS2), and fourth stage (MS3) collected microsclerotia at 24, 36, and 48 hpi, respectively, by scratching fungal tissue from the nylon membrane on PDA using a scalpel, and the fungal tissues were placed into a 2-mL screw cap prefilled with 1 mL sterile water and 1.0 mm zirconium dioxide beads. In order to remove hyphae and to obtain clean microsclerotia, the samples were gently vortexed using the Bioprep-BM24 instrument (Bioman Scientific Co., Ltd., New Taipei City, Taiwan) at 4.0 m/s speed for 20 s for MS1 samples, 5.0 m/s speed 30 s for MS2 samples, and 2 min without beads for MS3 samples. The samples were centrifuged at 14,000 rpm for 30 s, and the supernatants were discarded. The pellets were washed with 1 mL sterile water again before a centrifugation at 14,000 rpm for 1 min. The samples were assessed under a stereo dissecting microscope, and samples of good integrity and cleanness were immediately frozen in liquid nitrogen and stored in the −80°C freezer.

RNA-Seq preparation. The frozen samples were thawed by adding 1 mL of TRIzol (Invitrogen, Thermo Fisher Scientific Inc., Waltham, MA) and homogenized in a mortar with a pestle. The fungal nucleic acids were precipitated using isopropanol after cleaning by chloroform twice. The pellets were washed by 75% ethanol and resuspended in the UltraPure diethyl pyrocarbonate (DEPC)-treated water (Invitrogen). The fungal DNA was removed by the TURBO DNA-*free* kit (Invitrogen), and the fungal RNA was cleaned up and harvested by the RNA cleanup kit (Geneaid, New Taipei City, Taiwan) following the manufacturers' manuals. The integrity of purified RNA was qualified by the Bioanalyzer 2100 instrument (Agilent Technologies, Inc., Santa Clara, CA), and the library construction was completed using the Illumina MiSeq reagent kit v3 (Illumina, San Diego, CA). The 12 RNA libraries, which includes 3 biological replicates for the four stages of microsclerotia formation, were sequenced using the 150-bp single-end option of Illumina MiSeq (Illumina) in the Center of the Technology Commons (TechComm) in the College of Life Sciences at National Taiwan University.

Differential expression and gene ontology (GO) analyses. The Illumina raw data were quality control using the FASTQC and FASTX-Toolkit (63, 64). Reads with Phred scores above 30 were subjected to the gene expression quantification using the Kallisto version 0.46.1 and sleuth pipeline in default (65, 66). The genome of *M. phaseolina* AI-1 isolate was used as the reference (67). The differential gene expressions were analyzed by comparing the MS1, MS2, and MS3 stages to the MS0 stage, and the significance was determined at q value below 0.05. The expression patterns were clustered using the Pearson's distance and Ward.D2 method and visualized using the heat map function implemented in the R package "ComplexHeatmap" version 2.8.0 (68). The protein models of *M. phaseolina* AI-1 genome were annotated according to the OMA orthology database to obtain GO terms (69), and the GO enrichment analysis was analyzed using the R package "clusterProfile" version 4.1 (70). Venn diagram analyses were applied to identify the consensus genes with upregulation and downregulation in the MS1, MS2, and MS3 stages versus the MS0 stage, and the GO of consensus genes were subjected to REVIGO to visualize the functional annotation and statistical significance (71).

ROS inhibition assay. The ascorbic acid (PanReac AppliChem, ITW Reagents, Darmstadt, Germany), dithiothreitol (DTT) (BioShop Canada Inc., Burlington, Canada), and glutathione (BioShop) were freshly

prepared in the 9-cm petri dish PDA plates to minimize oxidation of the antioxidants. A 5-mm PDA block containing the mycelia edge of *M. phaseolina* was transferred to the center of the PDA plate, and the culture was continued in dark at 28°C until the mycelia covered the whole plate. The microsclerotia formation was examined and photographed under a stereo dissecting microscope at 240- to 300-fold magnitudes (WHITED Company Ltd., Taipei, Taiwan). Three photos were taken from each plate by photograph parameter adjustments, following exposure target 120, exposure time 41.66 ms, and gain 1006% of the RisingView 3.7 digital camera software, and all conditions (ascorbic acid, DTT, glutathione, and control) were repeated three times with three biological replicates/plates in each repeat. The images were input into ImageJ to quantify the microsclerotia amount using 8-bit grayscale transformation and set background threshold at 100, and then the particles were analyzed with the default settings for size (pixel^2) and circularity. The quantification data were analyzed in *R* environment version 4.0. Because the data fulfilled the assumption of normality and homoscedasticity based on the Shapiro-Wilk test and Breusch-Pagan test ($P > 0.05$), the data were analyzed using analysis of variance (ANOVA) and the Tukey honestly significant difference (HSD) test for mean separation.

In order to stain for O_2^- and H_2O_2, NBT (BioShop) was prepared in 70% dimethyl sulfoxide and 5× PBS buffer (51), while the DAB (AK Scientific Inc., Union City, CA) was prepared in double-distilled water (ddH_2O) via gradual acidification by 1 N HCl until the DAB powder was dissolved. The working concentration of both NBT and DAB was 0.05%, and the staining solution was passed through a 0.22-μm filter disk before storing at 4°C (48).

O_2^- and H_2O_2 stimulation assay and staining. The SOD1 inhibitor sodium diethyldithiocarbamate trihydrate (DETC) (Alfa Aesar, Thermo Fisher Scientific, Ward Hill, MA), and 30% vol H_2O_2 (PanReac AppliChem) were freshly prepared in the 9-cm petri dish PDA plates to minimize the reduction of oxidants, and the assay was conducted as described for the antioxidants. The microsclerotia formation was photographed and quantified as mentioned in the antioxidant assay. Two photos were taken from each plate, and all conditions (DETC, H_2O_2, and control) were repeated three times with three biological replicates/plates in each repeat. The data were checked for the assumption of normality and homoscedasticity ($P > 0.05$) before ANOVA and Tukey HSD test.

Data availability. The RNA-Seq raw data were deposited in the NCBI BioProject PRJNA752015.

SUPPLEMENTAL MATERIAL

Supplemental material is available online only.

SUPPLEMENTAL FILE 1, XLSX file, 0.9 MB.

SUPPLEMENTAL FILE 2, XLSX file, 0.01 MB.

SUPPLEMENTAL FILE 3, XLSX file, 0.4 MB.

SUPPLEMENTAL FILE 4, XLSX file, 0.5 MB.

SUPPLEMENTAL FILE 5, XLSX file, 0.5 MB.

SUPPLEMENTAL FILE 6, XLSX file, 0.02 MB.

SUPPLEMENTAL FILE 7, XLSX file, 0.03 MB.

SUPPLEMENTAL FILE 8, XLSX file, 0.01 MB.

ACKNOWLEDGMENTS

We thank the center of Technology Commons in the College of Life Science at National Taiwan University for providing Illumina sequencing supports.

This project was supported by grant MOST-108-2313-B-002-061-MY2 from the Ministry of Science and Technology, Taiwan (to H.-X.C.).

H.-H.L. and H.-X.C. conceived the project and established the experimental system. H.-H.L. completed the experiments for the RNA-Seq analyses and the ROS inhibition and stimulation assays. H.-H.L. and C.-C.H. completed the ROS staining. M.-N.T. and Y.-H.L. provided the fungal materials and reviewed the manuscript. H.-H.L. and H.-X.C. prepared the tables and figures, and H.-X.C. wrote the manuscript. All authors proofread the manuscript, and H.-X.C. supervised the project.

REFERENCES

1. Gupta GK, Sharma SK, Ramteke R. 2012. Biology, epidemiology and management of the pathogenic fungus *Macrophomina phaseolina* (Tassi) goid with special reference to charcoal rot of soybean (*Glycine max* (L.) Merrill). J Phytopathol 160:167–180. https://doi.org/10.1111/j.1439-0434.2012.01884.x.
2. Bandara AY, Weerasooriya DK, Bradley CA, Allen TW, Esker PD. 2020. Dissecting the economic impact of soybean diseases in the United States over two decades. PLoS One 15:e0231141. https://doi.org/10.1371/journal.pone.0231141.
3. Bradley CA, Allen TW, Sisson AJ, Bergstrom GC, Bissonnette KM, Bond J, Byamukama E, Chilvers MI, Collins AA, Damicone JP, Dorrance AE, Dufault NS, Esker PD, Faske TR, Fiorellino NM, Giesler LJ, Hartman GL, Hollier CA, Isakeit T, Jackson-Ziems TA, Jardine DJ, Kelly HM, Kemerait RC, Kleczewski NM, Koehler AM, Kratochvil RJ, Kurle JE, Malvick DK, Markell SG, Mathew FM, Mehl HL, Mehl KM, Mueller DS, Mueller JD, Nelson BD, Overstreet C, Padgett GB, Price PP, Sikora EJ, Small I, Smith DL, Spurlock TN, Tande CA, Telenko DEP, Tenuta AU, Thiessen LD, Warner F, Wiebold WJ, Wise KA. 2021. Soybean yield loss estimates due to diseases in the United States

and Ontario, Canada from 2015–2019. Plant Health Progress https://doi.org/10.1094/PHP-01-21-0013-RS.
4. Pawlowski ML, Hill CB, Hartman GL. 2015. Resistance to charcoal rot identified in ancestral soybean germplasm. Crop Sci 55:1230–1235. https://doi.org/10.2135/cropsci2014.10.0687.
5. Romero Luna MP, Mueller D, Mengistu A, Singh AK, Hartman GL, Wise KA. 2017. Advancing our understanding of charcoal rot in soybeans. J Integrated Pest Management 8:8. https://doi.org/10.1093/jipm/pmw020.
6. Mengistu A, Smith JR, Ray JD, Bellaloui N. 2011. Seasonal progress of charcoal rot and its impact on soybean productivity. Plant Dis 95:1159–1166. https://doi.org/10.1094/PDIS-02-11-0100.
7. Kaur S, Dhillon GS, Brar SK, Vallad GE, Chand R, Chauhan VB. 2012. Emerging phytopathogen *Macrophomina phaseolina*: biology, economic importance and current diagnostic trends. Crit Rev Microbiol 38:136–151. https://doi.org/10.3109/1040841X.2011.640977.
8. Willetts HJ, Bullock S. 1992. Developmental biology of sclerotia. Mycol Res 96:801–816. https://doi.org/10.1016/S0953-7562(09)81027-7.
9. Ainsworth GC, Bisby GR. 1950. A dictionary of the fungi. Commonwealth Mycological Institute, Kew, England.
10. Becker JG. 1956. Physico-chemical aspects of microsclerotia formation in *Verticillium albo-atrum* 9. PhD thesis, Purdue University, West Lafayette, IN.
11. Mathew F, Harveson R, Block C, Gulya T, Ryley M, Thompson S, Markell S. 2020. *Sclerotinia sclerotiorum* diseases of sunflower (white mold). Plant Health Instructor. https://www.apsnet.org/edcenter/disandpath/fungalasco/pdlessons/Pages/SclerotiniaSunflower.aspx.
12. Bolton MD, Thomma BPHJ, Nelson BD. 2006. *Sclerotinia sclerotiorum* (Lib.). de Bary: biology and molecular traits of a cosmopolitan pathogen. Mol Plant Pathol 7:1–16. https://doi.org/10.1111/j.1364-3703.2005.00316.x.
13. Lentz PL, McKay HH. 1970. Sclerotial formation in *Corticium olivascens* and other hymenomycetes. Mycopathol Mycol Appl 40:1–13. https://doi.org/10.1007/BF02128659.
14. Baard SW, Van Wyk PWJ, Pauer GDC. 1981. Structure and lysis of microsclerotia of *Verticillium dahliae* in soil. Trans Br Mycol Soc 77:251–260. https://doi.org/10.1016/S0007-1536(81)80027-7.
15. Smith RE. 1900. *Botrytis* and *Sclerotinia*: their relation to certain plant diseases and to each other. Bot Gaz 29:369–407. https://doi.org/10.1086/328001.
16. Purdy LH. 1979. *Sclerotinia sclerotiorum*: history, disease, and symptomatology, host range, geographic distribution, and impact. Phytopathology 69:875–880. https://doi.org/10.1094/Phyto-69-875.
17. Jagger IC. 1920. *Sclerotinia minor*, n. sp., the cause of a decay of lettuce, celery, and other crops, p 331–334. U.S. Department of Agriculture, Washington, DC. https://naldc.nal.usda.gov/catalog/IND43966303.
18. Griffiths DA. 1970. The fine structure of developing microsclerotia of *Verticillium dahliae* Kleb. Archiv Mikrobiol 74:207–212. https://doi.org/10.1007/BF00408881.
19. Coley-Smith JR, Cooke RC. 1971. Survival and germination of fungal sclerotia. Annu Rev Phytopathol 9:65–92. https://doi.org/10.1146/annurev.py.09.090171.000433.
20. Wyllie T, Brown M. 1970. Ultrastructural formation of sclerotia of *Macrophomina phaseolina*. Phytopathology 60:524–528. https://doi.org/10.1094/Phyto-60-524.
21. Georgiou CD, Patsoukis N, Papapostolou I, Zervoudakis G. 2006. Sclerotial metamorphosis in filamentous fungi is induced by oxidative stress. Integr Comp Biol 46:691–712. https://doi.org/10.1093/icb/icj034.
22. Georgiou CD. 1997. Lipid peroxidation in *Sclerotium rolfsii*: a new look into the mechanism of sclerotial biogenesis in fungi. Mycol Res 101:460–464. https://doi.org/10.1017/S0953756296002882.
23. Georgiou CD, Petropoulou KP. 2001. Role of erythroascorbate and ascorbate in sclerotial differentiation in *Sclerotinia sclerotiorum*. Mycol Res 105:1364–1370. https://doi.org/10.1017/S095375620100497X.
24. Georgiou CD, Zervoudakis G, Petropoulou KP. 2003. Ascorbic acid might play a role in the sclerotial differentiation of *Sclerotium rolfsii*. Mycologia 95:308–316. https://doi.org/10.2307/3762041.
25. Georgiou CD, Petropoulou KP. 2002. The role of ascorbic acid role in the differentiation of sclerotia in *Sclerotinia minor*. Mycopathologia 154:71–77. https://doi.org/10.1023/a:1015542916751.
26. Georgiou CD, Petropoulou KP. 2001. Effect of the antioxidant ascorbic acid on sclerotial differentiation in *Rhizoctonia solani*. Plant Pathol 50:594–600. https://doi.org/10.1046/j.1365-3059.2001.00608.x.
27. Georgiou CD, Tairis N, Sotiropoulou A. 2000. Hydroxyl radical scavengers inhibit lateral-type sclerotial differentiation and growth in phytopathogenic fungi. Mycologia 92:825–834. https://doi.org/10.2307/3761577.
28. Papapostolou I, Georgiou CD. 2010. Superoxide radical is involved in the sclerotial differentiation of filamentous phytopathogenic fungi: identification of a fungal xanthine oxidase. Fungal Biol 114:387–395. https://doi.org/10.1016/j.funbio.2010.01.010.
29. Papapostolou I, Georgiou CD. 2010. Hydrogen peroxide is involved in the sclerotial differentiation of filamentous phytopathogenic fungi. J Appl Microbiol 109:1929–1936. https://doi.org/10.1111/j.1365-2672.2010.04822.x.
30. Papapostolou I, Georgiou CD. 2010. Superoxide radical induces sclerotial differentiation in filamentous phytopathogenic fungi: a superoxide dismutase mimetics study. Microbiology 156:960–966. https://doi.org/10.1099/mic.0.034579-0.
31. Papapostolou I, Sideri M, Georgiou CD. 2014. Cell proliferating and differentiating role of H_2O_2 in *Sclerotium rolfsii* and *Sclerotinia sclerotiorum*. Microbiol Res 169:527–532. https://doi.org/10.1016/j.micres.2013.12.002.
32. Song Z, Yin Y, Jiang S, Liu J, Chen H, Wang Z. 2013. Comparative transcriptome analysis of microsclerotia development in *Nomuraea rileyi*. BMC Genomics 14:411. https://doi.org/10.1186/1471-2164-14-411.
33. Duressa D, Anchieta A, Chen D, Klimes A, Garcia-Pedrajas MD, Dobinson KF, Klosterman SJ. 2013. RNA-seq analyses of gene expression in the microsclerotia of *Verticillium dahliae*. BMC Genomics 14:607. https://doi.org/10.1186/1471-2164-14-607.
34. Luo X, Xie C, Dong J, Yang X. 2019. Comparative transcriptome analysis reveals regulatory networks and key genes of microsclerotia formation in the cotton vascular wilt pathogen. Fungal Genet Biol 126:25–36. https://doi.org/10.1016/j.fgb.2019.01.009.
35. Smirnoff N, Arnaud D. 2019. Hydrogen peroxide metabolism and functions in plants. New Phytol 221:1197–1214. https://doi.org/10.1111/nph.15488.
36. Weydert CJ, Cullen JJ. 2010. Measurement of superoxide dismutase, catalase and glutathione peroxidase in cultured cells and tissue. Nat Protoc 5:51–66. https://doi.org/10.1038/nprot.2009.197.
37. Chen ZX, Pervaiz S. 2010. Involvement of cytochrome *c* oxidase subunits Va and Vb in the regulation of cancer cell metabolism by Bcl-2. Cell Death Differ 17:408–420. https://doi.org/10.1038/cdd.2009.132.
38. Nolfi-Donegan D, Braganza A, Shiva S. 2020. Mitochondrial electron transport chain: oxidative phosphorylation, oxidant production, and methods of measurement. Redox Biol 37:101674. https://doi.org/10.1016/j.redox.2020.101674.
39. Sies H, Jones DP. 2020. Reactive oxygen species (ROS) as pleiotropic physiological signalling agents. Nat Rev Mol Cell Biol 21:363–383. https://doi.org/10.1038/s41580-020-0230-3.
40. Wang Y, Branicky R, Noë A, Hekimi S. 2018. Superoxide dismutases: dual roles in controlling ROS damage and regulating ROS signaling. J Cell Biol 217:1915–1928. https://doi.org/10.1083/jcb.201708007.
41. Zhang Z, Chen Y, Li B, Chen T, Tian S. 2020. Reactive oxygen species: a generalist in regulating development and pathogenicity of phytopathogenic fungi. Comput Struct Biotechnol J 18:3344–3349. https://doi.org/10.1016/j.csbj.2020.10.024.
42. Blokhina O, Virolainen E, Fagerstedt KV. 2003. Antioxidants, oxidative damage and oxygen deprivation stress: a review. Ann Bot 91:179–194. https://doi.org/10.1093/aob/mcf118.
43. Ilyas MB. 1976. Effect of soil fungicides on *Macrophomina phaseolina* sclerotium viability in soil and in soybean stem pieces. Phytopathology 66:355–359. https://doi.org/10.1094/Phyto-66-355.
44. Marquez N, Giachero ML, Declerck S, Ducasse DA. 2021. *Macrophomina phaseolina*: general characteristics of pathogenicity and methods of control. Front Plant Sci 12:634397. https://doi.org/10.3389/fpls.2021.634397.
45. Hou Y, Na R, Li M, Jia R, Zhou H, Jing L, et al. 2016. H_2O_2 is involved in cAMP-induced inhibition of sclerotia initiation and maturation in the sunflower pathogen *Sclerotinia sclerotiorum*. J Plant Pathol 99:17–26. https://doi.org/10.4454/jpp.v99i1.3771.
46. Kim H, Chen C, Kabbage M, Dickman MB. 2011. Identification and characterization of *Sclerotinia sclerotiorum* NADPH oxidases. Appl Environ Microbiol 77:7721–7729. https://doi.org/10.1128/AEM.05472-11.
47. Segmüller N, Kokkelink L, Giesbert S, Odinius D, van Kan J, Tudzynski P. 2008. NADPH oxidases are involved in differentiation and pathogenicity in *Botrytis cinerea*. Mol Plant Microbe Interact 21:808–819. https://doi.org/10.1094/MPMI-21-6-0808.
48. Marschall R, Tudzynski P. 2014. A new and reliable method for live imaging and quantification of reactive oxygen species in *Botrytis cinerea*: technological advancement. Fungal Genet Biol 71:68–75. https://doi.org/10.1016/j.fgb.2014.08.009.
49. Liu J, Yin Y, Song Z, Li Y, Jiang S, Shao C, Wang Z. 2014. NADH: flavin oxidoreductase/NADH oxidase and ROS regulate microsclerotium

development in *Nomuraea rileyi*. World J Microbiol Biotechnol 30:1927–1935. https://doi.org/10.1007/s11274-014-1610-7.
50. Vangalis V, Papaioannou IA, Markakis EA, Knop M, Typas MA. 2021. The NADPH oxidase A of *Verticillium dahliae* is essential for pathogenicity, normal development, and stress tolerance, and it interacts with Yap1 to regulate redox homeostasis. J Fungi 7:740. https://doi.org/10.3390/jof7090740.
51. Siegmund U, Heller J, van Kan JAL, Tudzynski P. 2013. The NADPH oxidase complexes in *Botrytis cinerea*: evidence for a close association with the ER and the tetraspanin Pls1. PLoS One 8:e55879. https://doi.org/10.1371/journal.pone.0055879.
52. Osato T, Park P, Ikeda K. 2017. Cytological analysis of the effect of reactive oxygen species on sclerotia formation in *Sclerotinia minor*. Fungal Biol 121:127–136. https://doi.org/10.1016/j.funbio.2016.11.002.
53. Xu L, Chen W. 2013. Random T-DNA mutagenesis identifies a Cu/Zn superoxide dismutase gene as a virulence factor of *Sclerotinia sclerotiorum*. Mol Plant Microbe Interact 26:431–441. https://doi.org/10.1094/MPMI-07-12-0177-R.
54. Yarden O, Veluchamy S, Dickman MB, Kabbage M. 2014. *Sclerotinia sclerotiorum* catalase SCAT1 affects oxidative stress tolerance, regulates ergosterol levels and controls pathogenic development. Physiol Mol Plant Pathol 85:34–41. https://doi.org/10.1016/j.pmpp.2013.12.001.
55. Huang Z, Lu J, Liu R, Wang P, Hu Y, Fang A, Yang Y, Qing L, Bi C, Yu Y. 2021. SsCat2 encodes a catalase that is critical for the antioxidant response, QoI fungicide sensitivity, and pathogenicity of *Sclerotinia sclerotiorum*. Fungal Genet Biol 149:103530. https://doi.org/10.1016/j.fgb.2021.103530.
56. Grintzalis K, Vernardis SI, Klapa MI, Georgiou CD. 2014. Role of oxidative stress in sclerotial differentiation and aflatoxin B1 biosynthesis in *Aspergillus flavus*. Appl Environ Microbiol 80:5561–5571. https://doi.org/10.1128/AEM.01282-14.
57. Zhang J, Wang Y, Du J, Huang Z, Fang A, Yang Y, Bi C, Qing L, Yu Y. 2019. *Sclerotinia sclerotiorum* thioredoxin reductase is required for oxidative stress tolerance, virulence, and sclerotial development. Front Microbiol 10:e00233. https://doi.org/10.3389/fmicb.2019.00233.
58. Rana K, Ding Y, Banga SS, Liao H, Zhao S, Yu Y, Qian W. 2021. *Sclerotinia sclerotiorum* Thioredoxin1 (SsTrx1) is required for pathogenicity and oxidative stress tolerance. Mol Plant Pathol 22:1413–1426. https://doi.org/10.1111/mpp.13127.
59. Veluchamy S, Williams B, Kim K, Dickman MB. 2012. The CuZn superoxide dismutase from *Sclerotinia sclerotiorum* is involved with oxidative stress tolerance, virulence, and oxalate production. Physiol Mol Plant Pathol 78:14–23. https://doi.org/10.1016/j.pmpp.2011.12.005.
60. Tian L, Li J, Huang C, Zhang D, Xu Y, Yang X, Song J, Wang D, Qiu N, Short DPG, Inderbitzin P, Subbarao KV, Chen J, Dai X. 2021. Cu/Zn superoxide dismutase (VdSOD1) mediates reactive oxygen species detoxification and modulates virulence in *Verticillium dahliae*. Mol Plant Pathol 22:1092–1108. https://doi.org/10.1111/mpp.13099.
61. Zhu Z, Yang M, Bai Y, Ge F, Wang S. 2020. Antioxidant-related catalase CTA1 regulates development, aflatoxin biosynthesis, and virulence in pathogenic fungus *Aspergillus flavus*. Environ Microbiol 22:2792–2810. https://doi.org/10.1111/1462-2920.15011.
62. Zhou J, Lin Y, Fu Y, Xie J, Jiang D, Cheng J. 2020. A cinnamyl alcohol dehydrogenase required for sclerotial development in *Sclerotinia sclerotiorum*. Phytopathol Res 2:13. https://doi.org/10.1186/s42483-020-00056-9.
63. Andrews S. 2010. FastQC: a quality control tool for high throughput sequence data. http://www.bioinformati/cs.babraham.ac.uk/projects/fastqc/.
64. Hannon GJ. FASTX-Toolkit. 2010. http://hannonlab.cshl.edu/fastx_toolkit.
65. Bray NL, Pimentel H, Melsted P, Pachter L. 2016. Near-optimal probabilistic RNA-seq quantification. Nat Biotechnol 34:525–527. https://doi.org/10.1038/nbt.3519.
66. Pimentel H, Bray NL, Puente S, Melsted P, Pachter L. 2017. Differential analysis of RNA-seq incorporating quantification uncertainty. Nat Methods 14:687–690. https://doi.org/10.1038/nmeth.4324.
67. Burkhardt AK, Childs KL, Wang J, Ramon ML, Martin FN. 2019. Assembly, annotation, and comparison of *Macrophomina phaseolina* isolates from strawberry and other hosts. BMC Genomics 20:802. https://doi.org/10.1186/s12864-019-6168-1.
68. Gu Z, Eils R, Schlesner M. 2016. Complex heat maps reveal patterns and correlations in multidimensional genomic data. Bioinformatics 32:2847–2849. https://doi.org/10.1093/bioinformatics/btw313.
69. Altenhoff AM, Škunca N, Glover N, Train C-M, Sueki A, Piližota I, Gori K, Tomiczek B, Müller S, Redestig H, Gonnet GH, Dessimoz C. 2015. The OMA orthology database in 2015: function predictions, better plant support, synteny view and other improvements. Nucleic Acids Res 43:D240–D249. https://doi.org/10.1093/nar/gku1158.
70. Wu T, Hu E, Xu S, Chen M, Guo P, Dai Z, Feng T, Zhou L, Tang W, Zhan L, Fu X, Liu S, Bo X, Yu G. 2021. clusterProfiler 4.0: a universal enrichment tool for interpreting omics data. Innovation 2:100141. https://doi.org/10.1016/j.xinn.2021.100141.
71. Supek F, Bošnjak M, Škunca N, Šmuc T. 2011. REVIGO summarizes and visualizes long lists of gene ontology terms. PLoS One 6:e21800. https://doi.org/10.1371/journal.pone.0021800.